Chemical Geology 719 (2026) 123579

Contents lists available at ScienceDirect

Chemical Geology

journal homepage: www.elsevier.com/locate/chemgeo

Thallium isotopic records of the Cambrian SPICE event reveal widespread deoxygenation and unique Mn-oxide cycling dynamics in early Paleozoic oceans

Matthew A. LeRoy [a,*], Benjamin C. Gill [a,b], Sean M. Newby [c], Theodore R. Them II [d], Jeremy D. Owens [e]

[a] Department of Geosciences, Virginia Polytechnic Institute and State University, Blacksburg, VA 24061, USA
[b] Global Change Center, Virginia Polytechnic Institute and State University, Blacksburg, VA 16 24061, USA
[c] Department of Earth and Planetary Sciences, University of Hong Kong, Hong Kong SAR, China
[d] Department of Geology and Environmental Geosciences, College of Charleston, Charleston, SC 29424, USA
[e] Department of Earth, Ocean and Atmospheric Science, National High Magnetic Field Laboratory, Florida State University, Tallahassee, FL 32306, USA

ARTICLE INFO

Editor: Vasileios Mavromatis

Keywords:
Thallium isotopes
SPICE Event
Mn-oxides
Anoxia
Paleoredox

ABSTRACT

Changes in the redox state of the oceans have exerted a powerful influence on the biological and chemical evolution of marine environments throughout Earth history. A relatively new proxy used to reconstruct this redox history is the analysis of the thallium isotopic composition (ε^{205}Tl) of fine-grained clastic rocks. Its utility stems from the central role and large fractionation that redox-sensitive Mn-oxides impart on the ε^{205}Tl of seawater in the modern ocean. Importantly, lower oxygenation levels of the ocean-atmosphere system earlier in Earth history may have fostered different Mn cycling dynamics and Tl isotope behavior. Here we explore this idea by examining a putative early Paleozoic interval of expanding marine deoxygenation, the Cambrian SPICE event (494.5 to 492.5 Ma). Our ε^{205}Tl records from two SPICE localities: the Alum Shale of Sweden and the Stockingford Shale Group of England suggest a rapid reduction of Mn-oxide sedimentation accompanied the initiation of the SPICE, consistent with expanding anoxia at this time. However, while both locations show broadly similar ε^{205}Tl patterns, to each other and to previous Tl investigations of anoxic events, we observe several differences that may reflect how Mn was cycled differently under lower oxygen levels. We note that most Mn-oxide sedimentation was likely localized in shallower environments creating more dynamic cycling of Mn and Tl than observed today. This view may have implications not only for the interpretation of Tl isotope data, but also for other isotopic systems influenced by Mn-oxides before the oxygenation of oceans reached modern levels.

1. Introduction

The stratigraphic record contains ample evidence that intervals of expanding and intensifying oceanic deoxygenation on a variety of timescales were a relatively common occurrence throughout Earth history with the well-documented Mesozoic Oceanic Anoxic Events (OAEs) being prime examples (Bond et al., 2013; Clarkson et al., 2015; Jenkyns, 2010; Wignall, 2001; Wignall and Twitchett, 1996; Zhang et al., 2020). Importantly, these episodes also appear to have dramatically affected Earth's chemical budgets and exerted significant influence upon the course of biological evolution (Bartlett et al., 2018; Kidder and Worsley, 2010; Ozaki and Tajika, 2013). Due to these critical effects, an important ongoing research aim is to better understand the magnitude, timing, and controls of these events. This effort remains challenging for the study of relatively ancient events (pre-Late Jurassic), because much of the sedimentary record pertaining to these intervals has been lost through subduction and other tectonic/metamorphic processes. Fortunately, there are a host of geochemical proxy records which suggest that the ancient record does contain examples of deoxygenation events—even in the absence of other more direct sedimentary evidence (e.g., widespread, coeval black shales) (Bond et al., 2013; Clarkson et al., 2016; Cui et al., 2021; Gill et al., 2011; Meyer et al., 2008; Thompson and Kah, 2012; Zhang et al., 2020). This recognition underscores the importance of leveraging geochemical proxies capable of providing

* Corresponding author.
E-mail address: mleroy@vt.edu (M.A. LeRoy).

https://doi.org/10.1016/j.chemgeo.2026.123579
Received 19 February 2026; Received in revised form 21 June 2026; Accepted 23 June 2026
Available online 24 June 2026

information about global oceanographic conditions from these limited sedimentary records. Especially critical to these efforts is the continuing development of proxies sensitive to the environmental redox conditions that develop when oxygen has been depleted, yet sulfate reduction has not initiated.

A relatively new approach used to track these conditions involves analyzing the Tl stable isotopic composition (ε^{205}Tl) of organic-rich, fine-grained clastic rocks (see Supplementary materials for an explanation of epsilon notation (ε)). Because the ε^{205}Tl compositions recorded in these rocks are strongly influenced by the global burial flux of redox-sensitive Mn-oxides in marine sediments, they ultimately record information about the integrated redox state of the oceans through time (Owens, 2019). This proxy has been used to investigate numerous intervals of marine deoxygenation including: the Late Ordovician mass extinction (LOME) (Kozik et al., 2023); the Lau event of the Silurian (Bowman et al., 2019); the Toarcian Stage of the Jurassic (T-OAE) (Them et al., 2018); the End-Permian Mass Extinction (EPME) (Newby et al., 2021); and, near the Cenomanian-Turonian Stage boundary in the Cretaceous (OAE-2, ~ 94 Ma) (Ostrander et al., 2017). These events revealed a similar pattern of systematic changes to the ε^{205}Tl of seawater. Fig. 1 provides a generalized summary of the key geochemical and biologic features shared by these deoxygenation events studied using Tl isotopes. Given the similar geochemical trends in carbon and sulfur isotopes (δ^{13}C and δ^{34}S, respectively) and trace metal enrichments observed for these deoxygenation episodes, we targeted the late Cambrian SPICE event (Steptoean Positive Carbon Isotope Excursion), as it shares many features in these same proxy records (Gill et al., 2021; Gill et al., 2011; LeRoy et al., 2021; LeRoy and Gill, 2019; Saltzman et al., 2011; Saltzman et al., 1998). Due to these similarities, in the present study we sought to investigate whether the SPICE affected the ε^{205}Tl of seawater in a similar manner as shown in these previous studies. Whether the SPICE is fundamentally different in its causes and consequences from these potentially similar events remains a question with important implications for understanding the co-evolution of Earth's marine environments and biosphere during the early Paleozoic.

1.1. The SPICE event

A large volume of data from numerous studies has established the SPICE as a global oceanographic event during which significant perturbations of the carbon (C), sulfur (S), uranium (U), and molybdenum (Mo) cycles occurred (Dahl et al., 2014; Gill et al., 2021; Gill et al., 2011; LeRoy et al., 2021; LeRoy and Gill, 2019; Saltzman et al., 2000; Saltzman et al., 1998; Sheng et al., 2026; Zhao et al., 2023). Furthermore, the initiation of these changes appears to have been temporally coupled with marine extinctions across several paleocontinents (Gerhardt and Gill, 2016; Saltzman et al., 2000; Yang et al., 2024)—raising the possibility of a common causal linkage between these features. This event occurred during the Paibian Age (~494.5 to 492.5 Ma) of the late Cambrian Furongian Epoch (Cothren et al., 2022; Farrell et al., 2025; Rooney et al., 2022) and is known from successions of this geologic age worldwide (Fig. 2). The SPICE itself is recorded as paired positive shifts in the isotopic composition of carbon- and sulfur-bearing materials (e.g., carbonate, organic matter, pyrite and sulfate) (Ahlberg et al., 2009; Gill

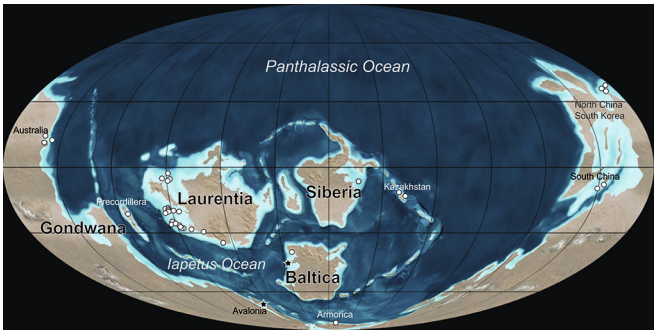

Fig. 2. Late Cambrian (~500 Ma) paleogeographic reconstruction (after Blakey, 2008), depicting the global distribution of locations where the SPICE event has been documented. The localities where we investigated thallium isotopes (ε^{205}Tl) for the present study are indicated by the position of the black stars in Avalonia (Stockingford Shale Group) and Baltica (Alum Shale).

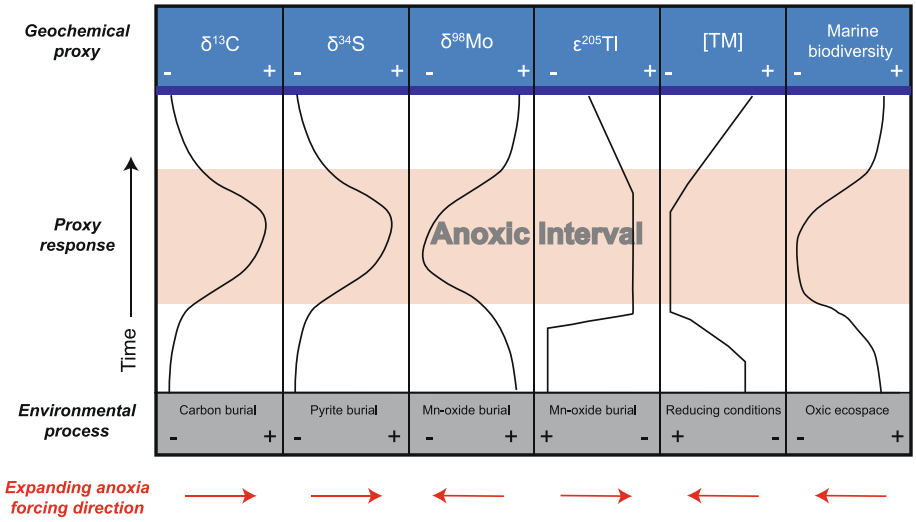

Fig. 1. Schematic depiction of the general geochemical and biological features of past intervals of oceanic anoxia explored using sedimentary thallium isotopes (ε^{205}Tl). The underlying environmental changes associated with this expanding anoxia appear to affect the isotopic composition of carbon (δ^{13}C), sulfur (δ^{34}S), molybdenum (δ^{98}Mo), and thallium (ε^{205}Tl) in seawater in a systematic, predictable pattern. Beyond these isotopic responses, these events also affect the seawater inventory of redox sensitive trace metals [TM] that are sequestered by and highly concentrated within reducing sediments. Shown below each proxy is its dominant controlling environmental process and the expected forcing direction induced by expanding anoxia (red arrows). Importantly, ε^{205}Tl rapidly tracks changes in the dynamics of Mn-oxide sedimentation driven by changes to the extent of oxygenated seafloor area. These initial changes revealed by ε^{205}Tl, consistently precede the anoxia-fostered enhanced carbon and sulfur burial which drives δ^{13}C and δ^{34}S to heavier values over the course of the events. Typically, it also appears that the intervals of highest extinction intensity are concentrated at these horizons where positive shifts in ε^{205}Tl indicate the most rapid expansion of reducing conditions. (For interpretation of the references to colour in this figure legend, the reader is referred to the web version of this article.)

et al., 2011; Peng et al., 2016; Saltzman et al., 2011; Woods et al., 2011). These isotopic trends have been attributed to an increase in the $\delta^{13}C$ and $\delta^{34}S$ of dissolved inorganic carbon and sulfate within the oceanic reservoir, reflecting the removal of large quantities of ^{12}C and ^{32}S from seawater through increased burial of organic carbon- and sulfur-bearing species (Dahl et al., 2014; Gill et al., 2011; Saltzman et al., 2000).

There remains some debate regarding the nuances of the relationship between the extinctions and the environmental conditions inferred by the geochemical proxy records of the SPICE, particularly whether they primarily reflect local forcings as opposed to being a globally synchronous event (Egenhoff et al., 2015; Schiffbauer et al., 2017; Wotte and Strauss, 2015). Currently, the most likely explanation for the co-occurrence of these features is through a global expansion of anoxic bottom waters shoreward during the early stages of the event (Gerhardt and Gill, 2016; Gill et al., 2011; LeRoy and Gill, 2019; Saltzman et al., 2000; Sørensen and Dahl, 2024; Zhao et al., 2023). This view is further strengthened by several complimentary studies which document the expansion of reducing conditions in: U isotopes (Dahl et al., 2014; Sheng et al., 2026); Mo isotopes and redox-sensitive trace metals (Gill et al., 2021); Mo and U isotopes (Zhao et al., 2023); trilobite diversity and Ce/Ce* data (Yang et al., 2024); compilations of Fe-speciation data (LeRoy et al., 2021); and minor sedimentary Hg enrichments (Pruss et al., 2019). Such an expansion of reducing conditions, as suggested by these studies, would have served to enhance the burial efficiency of organic matter and pyrite while simultaneously reducing the habitable seafloor area available to benthic metazoans—environmental changes consistent with the observed isotopic and biological patterns of the event. The long-term enhanced burial of these materials over the SPICE is also thought to have generated a net increase to atmospheric oxygen levels in its aftermath (Saltzman et al., 2011; Sheng et al., 2026; Zhao et al., 2023).

Testing this hypothesis remains challenging, however, as most paleoredox proxies are limited in their capacity to detect changes in the oxygenation state of the ocean at the global scale and are typically better suited for determining local to basin-scale redox conditions at the time of deposition (e.g., Fe speciation, trace metal enrichment records, etc.). While U and Mo isotopes have been employed to assess global-scale changes in marine redox conditions, the sensitivity of these proxies is often insufficient to reveal the earliest and/or more subtle changes in deoxygenation (e.g., non-sulfidic anoxia; see Owens, 2019) that are likely important environmental drivers of the biological and ecological trends of the SPICE and similar oceanographic events throughout Earth history (e.g., Sperling et al., 2015). Given these noted limitations, efforts have been underway to develop new approaches capable of assessing more subtle changes in local and global marine redox (e.g., Owens, 2019).

1.2. Thallium stable isotopes as a paleo-redox proxy

Recent work exploring novel metal isotope systems (e.g., U, Mo, V, Tl) to reconstruct ancient marine redox conditions have demonstrated potential to address some of the above shortcomings more effectively. Importantly, it has been observed that the ratio of the stable isotopes of Tl ($^{205}Tl/^{203}Tl$) preserved in organic-rich sediments accurately record the $\varepsilon^{205}Tl$ of overlying seawater in modern anoxic environments (Fan et al., 2020; Owens et al., 2017). This understanding coupled with the observation that the $^{205}Tl/^{203}Tl$ value of seawater is significantly influenced by redox-sensitive Mn-oxides, enables organic-rich, fine-grained rocks to reveal information about the prevalence of Mn-oxide sedimentation through time, and thus ultimately the global extent of marine (de)oxygenation.

Numerous studies of the contemporary geochemical cycle of Tl have established important constraints on the sources and sinks of Tl in modern seawater (see Owens (2019) and references therein for an overview). Several key features, outlined below, make the proxy well-suited for reconstructing ancient marine redox conditions. First, all the major inputs of Tl to seawater are isotopically similar to crustal/mantle values, exhibiting an $\varepsilon^{205}Tl$ value ~ -2. Furthermore, Tl in modern seawater is isotopically homogenous in unrestricted marine settings due to a sufficiently long residence time (~18 kyr) relative to oceanic mixing (~1.2 kyr) and its lack of utilization in biological processes (Nielsen et al., 2009; Ostrander et al., 2023; Owens et al., 2017; Rehkämper and Nielsen, 2004). A notable exception to this isotopic homogeneity is seen in the modern Black Sea, a restricted marine environment where Tl isotopic compositions distinct ($\varepsilon^{205}Tl$ value ~ -2) from the open ocean ($\varepsilon^{205}Tl$ value ~ -6) are observed. This different $\varepsilon^{205}Tl$ signature of the Black Sea is attributed to the local riverine input exerting the dominant influence on the dissolved Tl budget of the basin with limited contributions of Tl sourced from the open ocean where Mn oxide burial is the greater influence on isotopic composition. (Owens et al., 2017). This recognition highlights the need to consider the possibility of hydrographic restriction of a basin using any available depositional and stratigraphic contextual details when interpreting Tl isotopic data. Ideally, this complication can be alleviated by analyzing an event in sedimentary successions from more than one basin if possible.

The vast majority of the removal of Tl from seawater is principally controlled by two output fluxes with distinct isotopic compositions: low-temperature alteration of oceanic crust (AOC), which preferentially removes the light isotope (^{203}Tl) and adsorption onto authigenic Mn-oxide precipitates, which preferentially removes the heavy isotope (^{205}Tl) (Nielsen et al., 2017; Owens et al., 2017). Notably, the Tl removal flux due to AOC has a large magnitude with a small fractionation (~ -1.2), and the Mn-oxide removal flux has a large fractionation (up to $\sim +16.0$) while only accounting for around a third of the total Tl output from the ocean (updated in Newby et al. (2025)). Another removal pathway of particular importance for the use of Tl as a paleoredox proxy is through its association with authigenic pyrite in anoxic sediments. Importantly, this sink records the $\varepsilon^{205}Tl$ of ambient seawater without imparting any isotopic fractionation or significant drawdown of the marine Tl reservoir (Tl is unreactive toward sulfide unlike Mo, for example) making anoxic sediments an important archive of water column $\varepsilon^{205}Tl$ compositions. Sediments deposited under the most reducing anoxic conditions, euxinia, where there is free hydrogen sulfide in the water column were originally thought to provide the most accurate record of seawater $\varepsilon^{205}Tl$ compositions but subsequent work has established that ferruginous conditions (free Fe^{2+}) also provide equally accurate Tl records (Fan et al., 2020; Ostrander et al., 2020; Wang et al., 2022).

Perhaps most critically for investigating global marine redox, the precipitation and preservation (burial) of Mn-oxides requires oxygenated conditions from formation through early diagenesis as these phases undergo rapid dissolution when exposed to even mildly reducing conditions, ultimately leading to the recycling of Mn and any Tl adsorbed to these sediments (Newby et al., 2025; Wang et al., 2022). Consequently, the scavenging and sequestration of Tl from seawater by Mn-oxides only occurs where oxygenated conditions are present at the sediment/water interface (SWI) and through at least the upper portion of the sediment column. Due to this, an expansion of anoxic seafloor area is expected to reduce the magnitude of the Mn-oxide sink, thereby lessening the removal of ^{205}Tl from seawater, causing the residual oceanic reservoir to be enriched in this heavier isotope. It is also important to note that the various types of Mn-oxide sediments formed in different environments fractionate Tl to varying extents. For example, recent work by Clemente et al. (2025) suggest that the fractionation associated with Mn-oxides in shallow marine continental margin settings are more muted than those observed in deep marine environments.

Beyond the scavenging of Tl by Mn-oxide precipitates, the magnitude and composition of the other fluxes of Tl to and from seawater are thought to be relatively constant, or at least minimally impactful, over the short timescales relevant to the expansion of oceanic anoxia (millions of years or less (Owens, 2019)). Consequently, changes in the magnitude of the Mn-oxide removal flux are thought to be the main

influence on the ε^{205}Tl of seawater over similarly short timescales. Given these constraints, a large-scale expansion of reducing conditions at the seafloor is expected to be recorded as a positive directional shift in the ε^{205}Tl values of seawater— as the amount of seafloor area conducive to Mn-oxide formation and burial (oxygenated SWIs) decreases. Likewise, if the SPICE represents an interval of expanding anoxia, it should record a positive shift toward less negative ε^{205}Tl values as a result. This study aims to test this expectation by exploring the Tl isotope chemostratigraphy of the SPICE event in two paleogeographically distinct locations where the event has been previously studied.

2. Study background

During the late Cambrian the paleocontinents of Baltica and Avalonia were in the Southern Hemisphere, arranged along the eastern and southern margins of the Iapetus Ocean, respectively (Fig. 2). In Baltica, the stratigraphic interval spanning the SPICE can be found in the Alum Shale Formation of southern Scandinavia (Ahlberg et al., 2009). In Avalonia the time-equivalent Upper Cambrian interval can be found within the Stockingford Shale Group of the Nuneaton district of central England (Woods et al., 2011). Despite these successions being predominantly composed of organic-rich, fine-grained clastic rocks, deposition of each unit occurred under differing environmental conditions which may have influenced if and how primary changes in marine Tl isotopes were recorded at each site. Key aspects of these conditions are outlined below to provide context for our Tl isotope data with the aim of disentangling global oceanographic trends from local environmental effects and diagenesis.

2.1. The Alum Shale of southern Sweden

For this study, we investigated samples of the Alum Shale from the Andarum-3 drill core recovered from the Scania region of southern Sweden (55°42′55.75″N, 13°58′41.25″E). This drill core has been previously examined in several studies (Ahlberg et al., 2009; Gill et al., 2011; Gill et al., 2021), which provide important sedimentological, geochemical, and biostratigraphic context for the present investigation. This unit primarily consists of dark gray to black shales with a few minor limestone beds interspersed. Detailed information about the locality, paleontology, sedimentology, and carbon isotope stratigraphy of this drill core can be found in Figs. 2 & 3 of Ahlberg et al. (2009) and references therein. The deposition of the Alum Shale is interpreted to have occurred in the deeper portions of the Baltoscandian Basin, which had an open hydrographic connection to the adjacent Iapetus Ocean (Ahlberg et al., 2009; Dahl et al., 2019; Sturesson et al., 2005; Zhao et al., 2023). Environmental conditions appear to have remained relatively constant over several million years, from the middle Cambrian through early Ordovician producing a regionally-extensive succession of organic-rich, fine-grained clastic rocks deposited across much of southern Scandinavia (Nielsen and Schovsbo, 2015; Nielsen and Schovsbo, 2006; Schulz et al., 2021; Zhao et al., 2022). Iron speciation studies characterizing local water column redox conditions have shown that the Alum was deposited under persistent anoxia that became more reducing (see Fig. 3), transitioning from likely (Fe_{Py}/Fe_{HR} between 0.6

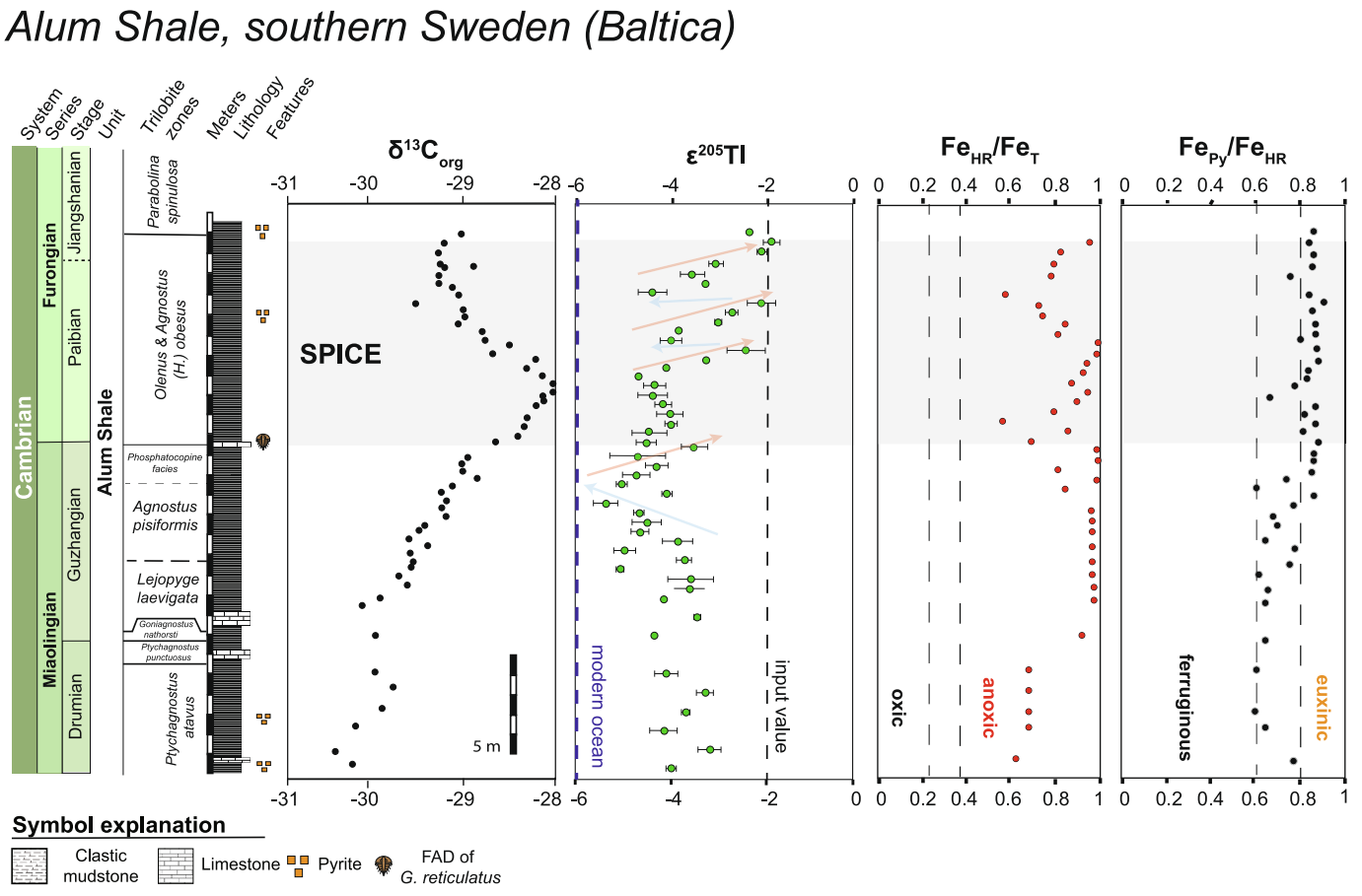

Fig. 3. Stratigraphic and geochemical profiles for the Alum Shale in the Andarum-3 core from Scania, Sweden. The thallium isotope data (ε^{205}Tl) from this study are displayed along with carbon isotopic ($\delta^{13}C_{org}$) and biostratigraphic data from Ahlberg et al. (2009), and iron speciation data (Fe_{HR}/Fe_T & Fe_{Py}/Fe_{HR}) from Gill et al. (2011). ε^{205}Tl values are displayed with 2σ error bars. Blue arrows on the ε^{205}Tl plot highlight shifts to more negative values and red arrows illustrate shifts to less negative values. These shifts are discussed in more detail in the main text (Sections 4.1 & 5.2). The gray shaded boxes depict the SPICE interval as identified in Ahlberg et al. (2009) and Gill et al. (2011). (For interpretation of the references to colour in this figure legend, the reader is referred to the web version of this article.)

and 0.8) to definitively euxinic conditions ($Fe_{Py}/Fe_{HR} > 0.8$), near the Guzhangian-Paibian Stage boundary (Gill et al., 2021; Gill et al., 2011). Notably, within this stratigraphic interval is where the initiation of the SPICE is generally recognized to occur across numerous globally-distributed sections (Saltzman et al., 2000). It also bears mentioning that while anoxia was the predominant state of the bottom waters in the Baltoscandian Basin there appear to have been many short-lived oxygenation episodes that allowed for brief, repeated colonization by benthic fauna, and yet were too short-lived to be recorded by the Fe-speciation proxy (Dahl et al., 2019). Additionally, Mo and U enrichment patterns in the Alum Shale suggest particulate shuttling by Mn-oxides was not occurring in this portion of the Baltoscandian Basin (see Fig. 4 in Gill et al., 2021), which provides further support for the idea that this location is likely to capture a faithful record of the ε^{205}Tl of seawater across the SPICE.

2.2. The Stockingford Shale Group of Central England

For this study we investigated a composite section of the Stockingford Shale Group that is composed of: two drill cores; Merevale boreholes — 1 (52.561735°N, 1.55977°W) and — 3 (52.558636°N, 1.548445°W); and two sections exposed at the Oldbury Quarry (52.551967, 1.544237°W; 52.560985°N, 1.551519°W), all located in the Nuneaton area of Warwickshire, in central England. Detailed information about this locality and its stratigraphic context, including paleontology, and carbon isotope stratigraphy can be found in Figs. 3 & 4 of Woods et al. (2011) and references therein. Generally, this unit is comprised of alternating intervals of organic-rich, sulfidic (dark gray) and organic-lean, sulfide-poor (light gray) siliciclastic mudrocks occasionally interrupted by cm-scale sand- and siltstone beds. Importantly for the purposes of this study, prior work on this succession (LeRoy et al.,

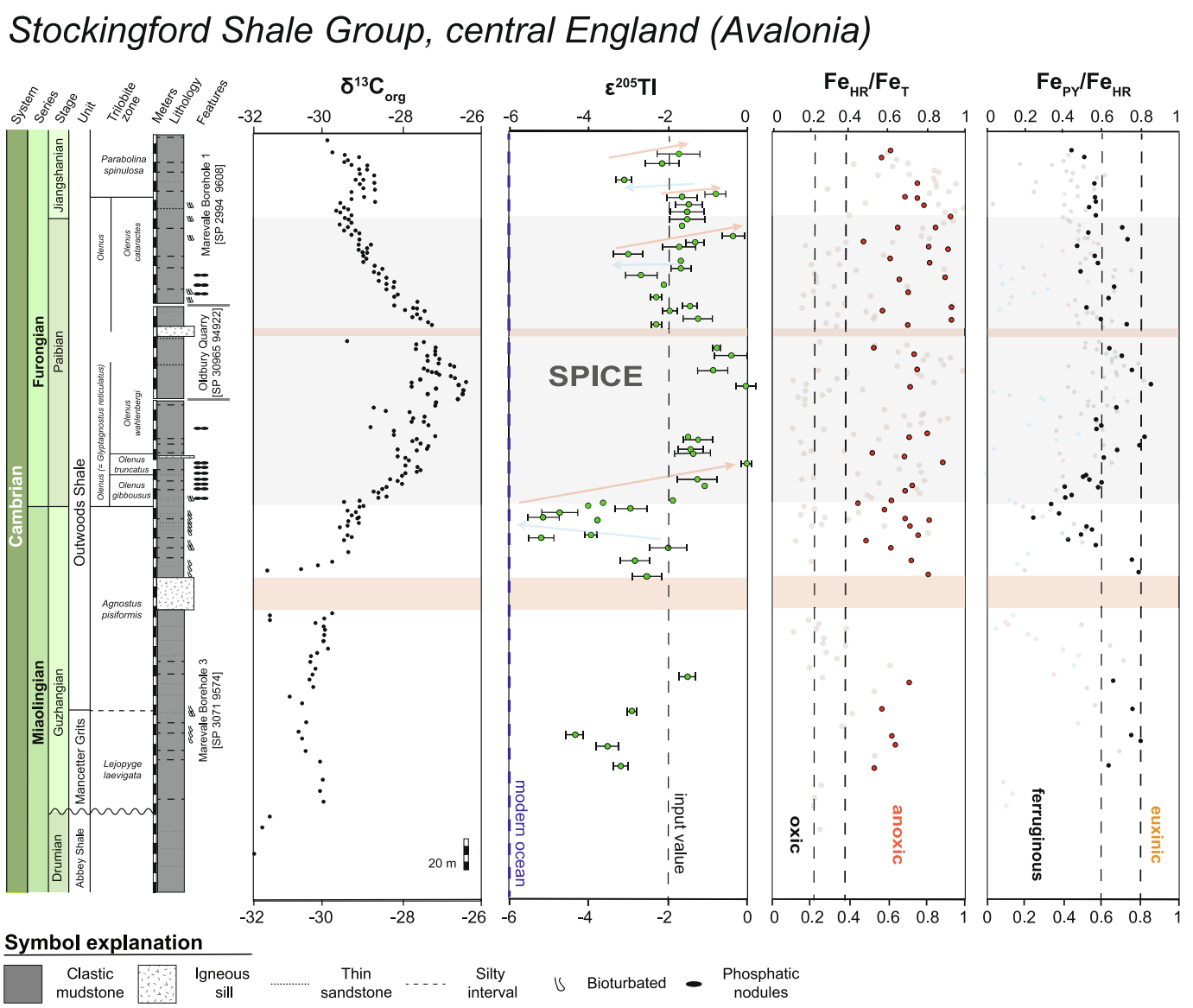

Fig. 4. Stratigraphic and geochemical profiles for the studied units of the Stockingford Shale Group (Merevale −1&3 cores) and Oldbury Quarry sections. The thallium isotope data (ε^{205}Tl) are from this study, while the carbon isotopic ($\delta^{13}C_{org}$) and biostratigraphic data are from Woods et al. (2011) and iron speciation data (Fe_{HR}/Fe_T & Fe_{Py}/Fe_{HR}) are from LeRoy et al. (2021). Lightly shaded circles represent iron speciation data for samples from LeRoy et al. (2021) that were not used in the present study, whereas fully shaded circles correspond to samples that were used for Tl isotopic analysis. ε^{205}Tl values are displayed with 2σ error bars. Blue arrows on the ε^{205}Tl plot highlight shifts to more negative values and red arrows illustrate shifts to less negative values. These shifts are discussed in further detail in the main text (Sections 4.2 & 5.2).The gray shaded boxes depict the SPICE interval as identified in Woods et al. (2011). The red shaded boxes illustrate the stratigraphic position of igneous sills that intruded during the Ordovician. (For interpretation of the references to colour in this figure legend, the reader is referred to the web version of this article.)

2021; Rushton, 1983; Rushton, 1978; Woods et al., 2011) provides a similar biostratigraphic and geochemical framework to the Alum Shale, enabling a detailed comparison of the Tl isotope records between each site.

In contrast to the depositional environment of the Alum Shale, the Stockingford Shale Group records an environment with higher overall rates of sediment accumulation during the same portion of the late Cambrian. Because of this, the expression of the SPICE in this succession is significantly thicker, spanning approximately 100 m compared to the 10s of meters seen in the Alum Shale (see Figs. 3 & 4 for comparison). Another key difference between the Stockingford Shale Group and the Alum Shale is the character of the local depositional redox environment as shown through previous Fe-speciation studies (Gill et al., 2021; Gill et al., 2011; LeRoy et al., 2021). Unlike the Alum Shale, where Fe data indicate persistent anoxia within the water column, the Stockingford Shale Group (Fig. 4) was deposited in a much more variable redox environment, recording fluctuations between oxic and anoxic conditions throughout (LeRoy et al., 2021). Despite this variability, the most common redox conditions recorded in the Stockingford Shale Group were ferruginous with only sparse, episodic development of euxinia (LeRoy et al., 2021). Perhaps most importantly when viewed together, the higher rates of sedimentation (proximity to clastic supply) and greater degree of redox variability (more influence of oxygenated surficial waters) seen in the Stockingford Shale suggest a more shoreward position within its depositional basin compared to the more distal interpretation favored for the Alum Shale. Ultimately, these differences in depositional environment have key implications for the interpretation of our Tl isotope data, and therefore are explored in greater detail in Section 5.1.

3. Methods

3.1. Materials and sampling

As mentioned above, this study leverages several previous efforts (Ahlberg et al., 2009; Gill et al., 2021; Gill et al., 2011; LeRoy et al., 2021; Woods et al., 2011) as a framework for investigating the Tl isotope chemostratigraphy of the SPICE event. Within this context, we generated new Tl isotopic data using splits of the bulk SPICE sample powders used for analyses in the aforementioned studies. Because these available samples and our subsequent analyses span a time interval that precedes and includes the SPICE, we were able to investigate changes in Tl isotopes over both the Guzhangian and Paibian Stages, allowing us to make inferences about the prevailing background state of the later Cambrian oceans and place the potential redox changes related to the SPICE within this broader temporal context.

3.2. Thallium isolation and isotopic analysis

Thallium was extracted from bulk sediment samples in the Geochemistry Group at the National High Magnetic Field Laboratory (NHMFL) at Florida State University (FSU) using the chemical extraction and purification protocol used by Nielsen et al. (2009). Briefly, this procedure liberates the Tl associated with authigenic mineral phases using 2 M nitric acid (HNO_3) and produces an aqueous solution containing the chemical constituents originally bound in these phases while leaving silicate phases undisturbed (to ensure any thallium within these phases is removed before further analysis). The supernatant liquid is then decanted and treated with aqua regia (concentrated HNO_3:HCl (1:3, *v*/v)) and concentrated hydrogen peroxide (H_2O_2) to break down any residual organic matter within the leachate. Thallium in the leachate is then isolated using the cation exchange column chromatography technique of Nielsen et al. (2009). Once isolated, thallium concentrations and the chemical purity (sufficient removal of Pb) of the leachates were analyzed by inductively coupled plasma mass spectrometry (ICP-MS) on an Agilent Quadrupole at the NHMFL at FSU. Samples that passed this screening procedure were deemed suitable for thallium isotopic analyses and were then analyzed on a Thermo Scientific Neptune multi-collector ICP-MS also housed at the NHMFL. The efficiency of the chemical extraction and purification techniques and instrumental accuracy and precision were monitored by replicate analyses of USGS shale reference SCO-1. These analyses recorded this reference standard at $\varepsilon^{205}Tl = -3.2 \pm 0.2$ ($N = 3$), within error of the long-term precision values of $\varepsilon^{205}Tl = -3.0 \pm 0.3$.

4. Results

4.1. Alum Shale thallium isotope chemostratigraphy

Fig. 3 displays our thallium isotope ($\varepsilon^{205}Tl$) data for the Alum Shale. These data are displayed within the stratigraphic and geochemical context provided by the previous carbon isotope ($\delta^{13}C_{org}$) and iron speciation (Fe_{HR}/Fe_T and Fe_{Py}/Fe_{HR}) data reported by the studies of Ahlberg et al. (2009) and Gill et al. (2011), respectively. Thallium isotopes display a range of ~3.5 ε units, (between −5.4 and − 1.9 $\varepsilon^{205}Tl$) over the investigated stratigraphy. The lowest portion of the Alum sampled here spans the *Ptychagnostus atavus* through the *Lejopyge laevigata* trilobite biozones (upper Drumian through lower Guzhangian) and record $\varepsilon^{205}Tl$ values that vary between roughly −4.4 and − 3.6. Above this, within the *Agnostus pisiformis* zone (upper Guzhangian), values decrease toward −5.4 before beginning a protracted positive shift to a value of −3.6 across the interval just prior to and during the initial phase of the SPICE (spanning the Guzhangian/Paibian Stage boundary). Above this, within the *Olenus & Agnostus obesus* zone $\varepsilon^{205}Tl$ values remain relatively constant around −4 through the rising limb and peak $\delta^{13}C$ values of the SPICE. Following this, within the falling limb of the carbon isotope excursion (CIE), $\varepsilon^{205}Tl$ values show three positive shifts spanning around 2 ε-units between roughly −4 and − 2 which comprise the remaining portion of the Paibian Stage (*Olenus & Agnostus obesus* zones). The least negative values are encountered at the top of the core within the *Parabolina spinulosa* zone (upper Paibian/lower Jiangshanian), an interval that occurs just after the end of the SPICE as defined in Ahlberg et al. (2009).

4.2. Stockingford Shale Group thallium isotope chemostratigraphy

Our Tl isotope results for the Stockingford Shale Group are presented in Fig. 4. For these analyses, we measured $\varepsilon^{205}Tl$ on a subset of samples of the Stockingford that were used for the Fe-speciation study of LeRoy et al. (2021). From these, we selected 52 samples deemed suitable for analysis using the following criteria: anoxic depositional conditions ($Fe_{HR}/Fe_T > 0.38$); TOC content above 1 wt%; and a sufficiently high proportion of the reactive iron pool present in pyrite (i.e., Fe_{Py}/Fe_{HR} values above 0.5, with the highest ratios preferentially selected). Overall, our samples record a range of 5.1 ε-units spanning from −5.2 to −0.1. The lower portion of the Merevale-3 core within the *Lejopyge laevigata* trilobite biozone (lower Guzhangian Stage) record $\varepsilon^{205}Tl$ values between −4.4 and − 2.9. Above this, in the upper portions of the *Agnostus pisifomis* trilobite biozone (upper Guzhangian Stage), $\varepsilon^{205}Tl$ steadily shifts to more negative values decreasing from −2.0 to −5.2 in the interval just preceding the initiation of the SPICE (as defined in Woods et al. (2011)). This decreasing $\varepsilon^{205}Tl$ trend is then reversed across the *Olenus gibbousus* trilobite zone (lowermost Paibian Stage) with values becoming progressively less negative, quickly rising from −5.2 to −1.1. Importantly, this stratigraphic interval of increasing $\varepsilon^{205}Tl$ also records the positive shift in carbon isotopes that marks the initiation of the SPICE. In the uppermost portion of the Merevale-3 core, which spans the *Olenus truncatus* through the *Olenus wahlenbergi* trilobite zones and falls within the rising limb of the SPICE, $\varepsilon^{205}Tl$ remains fairly constant with values around −1.5. Above this, within the Oldbury Quarry portion of the stratigraphy, values steadily decrease from an initial value of −0.1 to −2.0 up section. The uppermost stratigraphy studied is found in the

Merevale-1 core, which includes the *Olenus cataractes* through the *Parabolina spinulosa* trilobite zones (Paibian through lower Jiangshanian Stages). Through this core, ε^{205}Tl values range between roughly −3.1 and − 0.3 with most samples recording values fluctuating around −1.5. Within this broad framework, three separate small positive shifts of around 1.5 ε-units can be discerned. Two of these occur within the falling limb of the SPICE (*Olenus cataractes* Zone) and a third occurs within the *Parabolina spinulosa* trilobite zone in an interval identified as "excursion 2" by Woods et al. (2011) based on a second, smaller (~ 1‰), post-SPICE CIE they observed.

5. Discussion

5.1. Potential effects of local depositional redox conditions upon thallium isotope signatures

Iron speciation data from the Stockingford Shale Group (Fig. 4) reported by LeRoy et al. (2021) reveal two important differences between the local redox conditions at the site in Avalonia and those observed for the Alum Shale study location in Baltica by Gill et al. (2021, 2011): (1) Seafloor conditions were predominantly anoxic but significant fluctuations in water column redox, spanning oxic through euxinic conditions, occurred, and (2) when anoxic conditions occurred, they were largely ferruginous with only sparse, episodic intervals of euxinia. These features contrast with the persistently anoxic and dominantly euxinic conditions recorded throughout most of the Alum Shale (Fig. 3). While these differences in local redox environment could potentially affect the preserved Tl isotope signatures we document here, we are confident that our sample selection (see section 4.1) ensure a faithful record of the ε^{205}Tl of seawater was preserved in our samples as all were deposited under anoxic water columns and contain limited Mn content (Wang et al., 2022)—thereby constituting a conservative application of the proxy. Importantly, it has been observed that sediments in modern ferruginous settings accurately capture the ε^{205}Tl of overlying seawater and this insight has been subsequently applied to ancient deposits to reconstruct global Tl dynamics using data from ferruginous basins (Fan et al., 2020; Ostrander et al., 2020; Wang et al., 2022). The suitability of using ferruginous samples is further supported by a comparison of our ε^{205}Tl results from the Stockingford samples when grouped into ferruginous ($Fe_{Py}/Fe_{HR} < 0.6$) and euxinic ($Fe_{Py}/Fe_{HR} > 0.6$) populations. If these different redox environments recorded in the Stockingford samples affected the Tl isotope compositions in a systematic manner, we might expect to see consistently offset ε^{205}Tl values between the ferruginous and euxinic sample populations. This is not the case, however, as can be seen in Supplemental Figs. 1 & 2 (Figs. S1 & S2), which indicate no significant difference between the ε^{205}Tl of samples whether designated euxinic or ferruginous. Given these arguments, we feel confident that the Tl isotopic analyses of ferruginous samples used in this study also likely captured a faithful record of seawater ε^{205}Tl values across the study interval (Newby et al., 2025).

The variable redox conditions seen in the Stockingford Shale Group presents another potential complication that could have affected our Tl results. It is possible that Tl initially sequestered on Mn-oxides during oxic intervals could later be remobilized by reductive dissolution of these particles within anoxic porewaters of the sediment column. This remobilized Tl could then be incorporated into overlying intervals deposited under anoxic conditions and mix with Tl directly derived from seawater, ultimately shifting the ε^{205}Tl of these sediments to more ^{205}Tl enriched compositions (Fan et al., 2020; Newby et al., 2025). If Tl adsorption only occurs onto pyrite, as is currently understood (Nielsen et al., 2011), then it would be required that Mn reduction occurs in close proximity to sulfate reduction to capture such an isotope value—to date, this has not been observed in modern environments (Fan et al., 2020; Newby et al., 2025; Owens et al., 2017). To explore this possibility, we examined our results with respect to the proximity of each sample to the nearest intervals of oxic deposition that could serve as source beds for remobilized diagenetic fluids (Fig. S3). This process, if in operation, is presumed to have occurred in a similar manner as the remobilization documented for other redox-sensitive elements in Owens et al. (2012). If these underlying beds were a source of remobilized Tl, we would expect a negative correlation in the plot shown in Fig. S3, as samples with closer proximity to oxic beds would likely be more prone to such an effect and should be associated with less negative ε^{205}Tl values. This analysis showed no discernible relationship between the reported ε^{205}Tl values and the proximity of underlying intervals of oxic sedimentation ($r^2 = 0.041$), therefore, this suggests this process has not significantly affected our Tl isotope data. Given these considerations, we are confident our data reflect primary changes in the ε^{205}Tl of seawater at the time of deposition and are not an artifact of later diagenetic processes. Despite the above arguments in favor of the potential for the Alum Shale and Stockingford Shale Group sediments to faithfully record $\varepsilon^{205}Tl_{SW}$, these records do show notable differences in the absolute value and magnitude of changes in ε^{205}Tl, despite displaying similar overall trajectories across the rising and falling limb of the SPICE. These differences are explored in more detail below.

5.2. Thallium isotopic record of the SPICE

Overall, our Tl isotope data suggest that the Tl cycle in the Cambrian oceans was characterized by a smaller flux of Mn-oxide burial relative to the modern ocean as has also been suggested for the early Cambrian Age 2-Age 3 transition (Clemente et al., 2025). Evidence for this difference is seen in pre-SPICE ε^{205}Tl values across the Guzhangian that fall between −4.4 and − 3.2 at each location (Figs. 3 & 4)—values less negative than observed in the modern oceans (ε^{205}Tl = −6.0). While these values could reflect potential differences in the magnitude or composition of any of the fluxes of Tl to or from seawater, a host of proxy data and modeling studies support the notion of a less-oxygenated marine environment at this time (Cole et al., 2020; Gill et al., 2021; Gill et al., 2011; LeRoy et al., 2021; Lu et al., 2018; Pruss and Gill, 2024; Saltzman et al., 2015; Sperling et al., 2015). Therefore, it is reasonable to expect that the magnitude of the Mn-oxide burial flux would also be smaller due to these lower marine oxygen levels, resulting in a less negative ε^{205}Tl of seawater relative to the modern ocean.

These less-oxygenated Cambrian oceans also appear to have influenced how the increased anoxia seen during the SPICE influenced the marine Tl cycle. This response appears unique in systematic ways when compared to more recent anoxic episodes such as OAE-2 (Ostrander et al., 2017), the T-OAE (Them et al., 2018) the EPME (Newby et al., 2021), the Lau Event (Bowman et al., 2019), and the LOME (Kozik et al., 2023). Generally, during these anoxic episodes ε^{205}Tl shifted toward less negative values prior to the associated positive CIEs and remained less negative relative to the pre-event baseline after the CIE maxima and (inferred) peak of enhanced carbon burial (see Fig.1 for an illustration of this general relationship). Our Tl isotope data (Figs. 3 and 4), while broadly consistent with this pattern, do display important differences. Similarly to these previous studies, our data show ε^{205}Tl shifting toward less negative values during the early stages of the SPICE (CIE) suggesting an expansion of reducing conditions and a decline in the magnitude of the Mn-oxide sink. However, both SPICE records also display a pronounced negative shift in ε^{205}Tl that occurs near but just prior to the onset of the CIE. This negative shift occurs within the *Agnostus pisifomis* trilobite zone at each location (Guzhangian Stage), however its magnitude and relative stratigraphic level within the biozone differs between the sites. In the Stockingford Group it spans slightly more than 3 ε-units, decreasing from −2.0 to −5.2 over the upper quarter of the *Agnostus pisifomis* zone (~20 m). In contrast, the negative shift in the Alum Shale is a little less than 2 ε-units (−3.6 to −5.4) and instead occurs over the middle portion of the *Agnostus pisifomis* biozone (~3 m). It bears mentioning that a similar negative shift in ε^{205}Tl has been reported for some sections during the early phase of the CIE for the Toarcian Oceanic Anoxic Event, end-Permian mass extinction, and Late

Ordovician mass extinction, respectively (Kozik et al., 2023; Newby et al., 2021; Them et al., 2018).

Whether these apparent differences in timing are an artifact of the available biostratigraphic resolution, differences in sediment accumulation rates across the biozone, or reflect a real temporal offset in the isotope records between the two sections is currently unclear. However, given the short residence time and conservative distribution of Tl in the modern ocean, along with the position of the ε^{205}Tl shifts relative to the carbon isotope profiles, it is presumed that these changes were likely coeval between the two sections despite the noted uncertainties in biostratigraphic zonation in particular. Even given these considerations there are still important differences between each ε^{205}Tl record that require further discussion. Most notably, the prominent difference in the magnitude and absolute values of the ε^{205}Tl shifts at each site during the SPICE onset requires a conceptual model that can explain these discrepancies and account for the negative ε^{205}Tl excursions in the phase just prior to the event. Importantly, the overarching pattern of isotopic response shared by and unique to these SPICE records, compared to more recent anoxic episodes explored using Tl isotopes, may stem from key differences between the late Cambrian oceans and the more familiar dynamics of Tl cycling in the modern ocean, which underpin the current understanding of marine Tl isotope behavior. In the following section we specifically explore how the main locus of Mn-oxide generation and preservation in the late Cambrian oceans may have been different and how this could impart some of the unique features of the Tl records we present here.

5.3. *The locus of manganese-oxide burial during the early Paleozoic*

The shift toward more negative ε^{205}Tl values at each study site during the latest Guzhangian Age (Figs. 3 & 4) fundamentally records a relative increase in the removal rate of ^{205}Tl from seawater, suggesting an enhanced Mn-oxide burial flux just prior to the initiation of the SPICE. This observation presents two possible scenarios that could account for this rapid increase in global Mn-oxide burial: (1) either there was an increase in the geographic extent of oxygenated bottom waters and an attendant increase in the spatial extent and magnitude of the Mn-oxide sink, or (2) there was an increase in the supply of Mn to already oxygenated waters that increased the rate of new Mn-oxide generation. The first possibility seems an unlikely scenario given that the available body of proxy data, including C, Mo, and U isotopes, largely suggest that reducing environments were expanding near the onset of the SPICE (Dahl et al., 2014; Gill et al., 2021; Gill et al., 2011; Landing, 1983; LeRoy et al., 2021; LeRoy and Gill, 2019; Pruss et al., 2019; Saltzman et al., 2000; Sheng et al., 2026; Sørensen and Dahl, 2024; Yang et al., 2024). Given these constraints, the latter possibility bears further exploration, and therefore we will consider mechanisms that could have supplied increased amounts of dissolved Mn (Mn^{2+}) to oxygenated waters and thereby increased the burial rate of Mn-oxides.

There are several features unique to Cambrian (and more ancient) oceans, relative to the modern and later Paleozoic, that may have may have facilitated such a process. Recent estimates, based upon modeling and available proxy data, bracket the likely range of Cambrian pO_2 levels between 10 and 40% of present atmospheric levels (Krause et al., 2018; Sperling et al., 2015). At these lower levels of atmospheric oxygen, modeling efforts indicate that the deeper ocean would have been less oxygenated and potentially even fully anoxic (Canfield, 1998; Stolper and Keller, 2018). Critically, this view is increasingly in line with the growing body of geochemical proxy data which suggest the full ventilation of the deeper oceans likely occurred in the later Paleozoic (Dahl et al., 2010; Lu et al., 2018; Ostrander et al., 2025; Sperling et al., 2015), and recent Tl isotope data from the earlier Cambrian also provide further support for this concept (Clemente et al., 2025). Most relevant to the present discussion, in a less oxygenated ocean the precipitation of Mn-oxides would be limited or entirely precluded from broad areas of the deep ocean floor where they occur extensively today. Notably, these poorly oxygenated, deeper water masses would also likely contain appreciable concentrations of dissolved Mn (and Fe) sourced from reducing hydrothermal and benthic fluids. Given this scenario, it is likely that shallow shelf environments served as a more important locus of Mn-oxide precipitation and burial—in contrast to the deeper environments where significant quantities of Mn-oxide-rich sediments form and are buried today (Hein and Koschinsky, 2014). If this were the case, this shallower locus for Mn-oxide formation would be highly sensitive to oceanographic processes that could impact the geographic extent of oxygenated seafloor along the margins of the continents such as changes in sea level, oceanic circulation, and or primary productivity. However, dissolved oceanic concentrations of both Mn and Fe may also be controlled by authigenic mineral phases—Mn carbonates, phosphates, clays, and pyrite—on a global scale that allows for significant removal of these metals from seawater without necessitating accumulation exclusively in shallow oxic sediments. Recent studies suggest some of these authigenic minerals were more important sinks of these elements in the Cambrian (Hagen et al., 2024; Pruss and Gill, 2024) but further work is necessary to establish whether authigenic-rich horizons in Cambrian strata were an important limiting factor in pre-SPICE availability of these metals.

To illustrate this, Figs. 5A & B show a schematic diagram of how the dynamics of Mn-oxide burial and the ε^{205}Tl of seawater are expected to be affected by changing sea-level and expanding anoxic bottom waters under these two different oceanographic scenarios. The first scenario, depicted in Fig. 5A, shows these dynamics in a fully ventilated ocean within a region akin to a modern ocean oxygen minimum zone (OMZ) where highly productive surface waters lead to depletion of dissolved O_2 at depth. Likewise, Fig. 5B represents an alternative scenario where lower atmospheric pO_2 renders the deep oceans largely oxygen deficient and consequently Mn-oxide precipitation predominantly occurs in shallow, oxygenated nearshore waters. In each scenario the initial expansion of reducing conditions across the shelves would dissolve and mobilize previously buried Mn-oxides enriched in ^{205}Tl, however the effect of this remobilized ^{205}Tl on the seawater ε^{205}Tl value is expected to be more pronounced in the scenario presented in Fig. 5B— as the volume of shallow water Mn-oxide sediments subjected to dissolution would be far greater. A critical difference between these scenarios lies in the overall supply of dissolved Mn made available to form *new* Mn-oxides as anoxia expands shoreward. Importantly, this type of shoreward expansion of anoxic waters has recently been implicated as a key feature of the SPICE event (Sørensen and Dahl, 2024; Yang et al., 2024). It is noteworthy that in the scenario depicted in Fig. 5A there is no net increase in the transfer of Mn to oxygenated waters, while in Fig. 5B a *larger* pool of Mn, from poorly oxygenated deep waters, is available to be advected to shallow, oxygenated waters where new Mn-oxides could rapidly form. This is an especially important consideration given the observation that Mn-oxides formed in shallow shelf regions of the modern ocean—such as the Baltic Sea—precipitate and grow by orders of magnitude more rapidly (up to 20 mm/kyr), than those formed in the deep sea (1–5 mm/My) (Hlawatsch et al., 2002; Koschinsky and Hein, 2017). It has also been observed recently that these shallow-shelf Mn-oxide sediments impart a smaller fractionation in Tl isotopes than the more slowly accumulating deep-sea nodules and crusts (Clemente et al., 2025). It is therefore reasonable to expect that in Cambrian and more ancient oceans, rapid, shallow-water Mn-oxide formation could occur extensively during interactions between Mn-rich anoxic water masses and the oxygenated surface waters during changes in circulation, upwelling, or sea-level. This rapid Mn-cycling could also affect the residence time and isotopic distribution of Tl (i.e., increase heterogeneity) within different portions of the global ocean in ways unique from modern Tl cycling.

These new Mn-oxides formed near the chemocline between oxygenated upper ocean and anoxic deeper waters expanding shoreward would then provide a new local sink for ^{205}Tl and foster the development of a ^{205}Tl-depleted global water mass (ε^{205}Tl ≈ -6 in seawater recorded

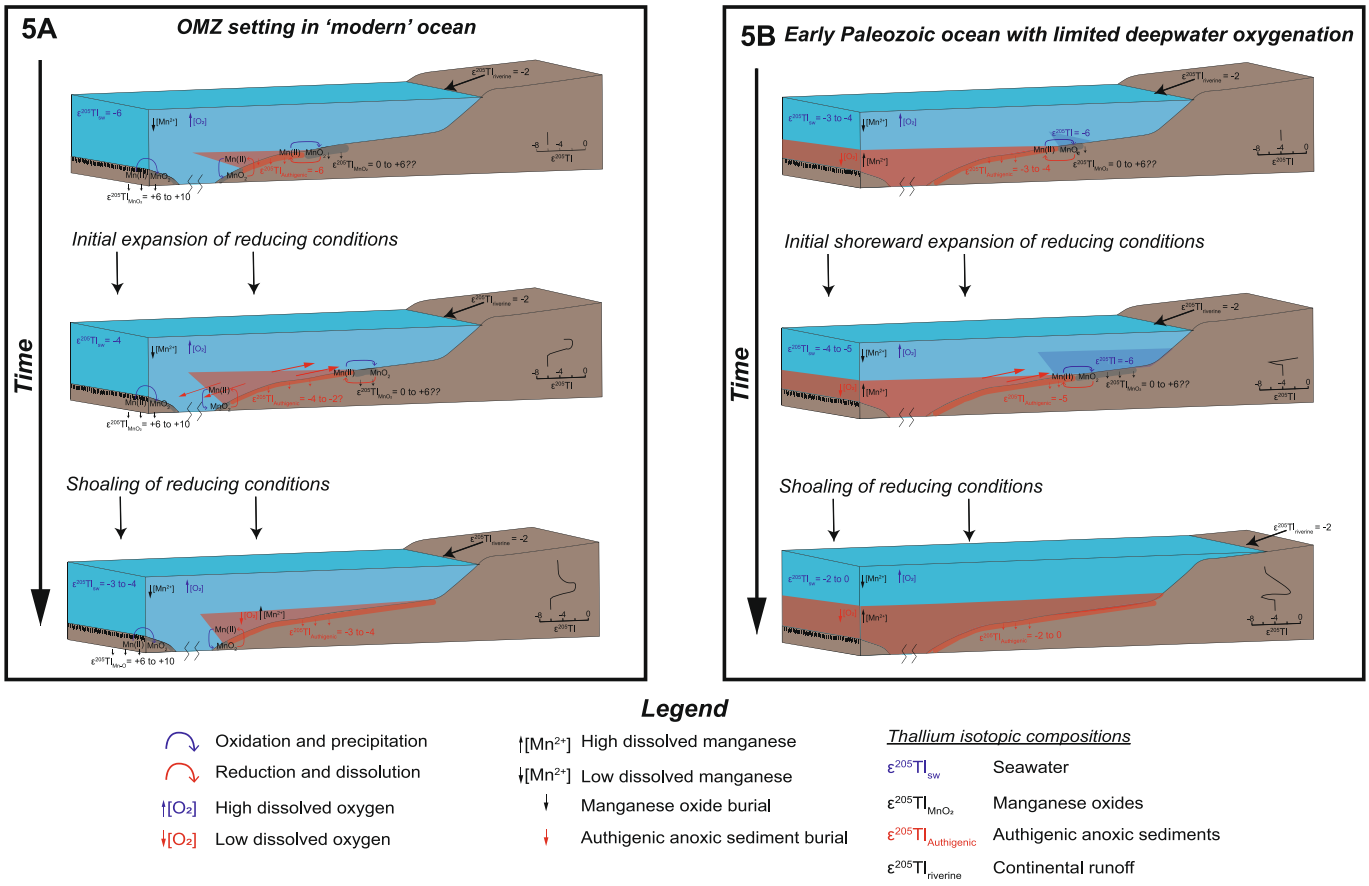

Fig. 5. Generic basin profiles depicting two scenarios for the impact of expanding anoxia on Mn-oxide sedimentation and the response of the Tl isotope proxy under these different oceanic redox regimes. 5 A includes deep waters that are fully oxygenated and serve as a significant locus of Mn-oxide sedimentation, as is the case in the oceans today. Likewise, 5B represents an alternative scenario where lower atmospheric pO_2 renders the deep oceans largely anoxic, and consequently Mn-oxides only precipitate in shallow waters where atmospheric oxygen penetrates sufficiently. See Section 5.3 for further details.

by sediments in the wedge in Fig. 5B). This process would serve to shift the ε^{205}Tl of nearby anoxic, authigenic sediments to more negative values during the initial expansion of anoxia shoreward, a result which contrasts with the shift to less negative values a similar expansion of anoxic waters would induce in a well-oxygenated ocean (scenario depicted in Fig. 5A). This initial negative shift is eventually supplanted by steadily increasing ε^{205}Tl values as anoxia engulfs increasingly large areas of the shelf causing the dissolution of existing shallow water Mn-oxides, releasing ^{205}Tl to seawater, in addition to progressively precluding the formation and burial of new Mn-oxides further enriching the Tl isotopic composition of seawater. As reducing conditions begin to dissipate this dynamic would be reversed and these same shallow shelf regions would serve as an important sink for ^{205}Tl as Mn-oxide formation and burial is reestablished. In this scenario, it is likely that the expansion and contraction of reducing conditions could rapidly alter the ε^{205}Tl of the local water mass which would ultimately be recorded as directional shifts in the ε^{205}Tl of authigenic, anoxic sediments deposited nearby within the basin. We see potential evidence for this dynamic in the sets of directional shifts during the falling limb of the SPICE in both the Alum Shale and the Stockingford Shale Group (Figs. 3 & 4). Furthermore, it bears mentioning that the scenario shown in Fig. 5B would also be sensitive to relatively small changes in sea level, water mass restriction, and ocean circulation—a notable consideration given the higher sea levels and extensive epicontinental seas characteristic of the Cambrian. Importantly, this localized heterogeneity is an expected outcome of the relatively higher levels of dissolved Mn in the anoxic waters of the scenario depicted in Fig. 5B. In the scenario shown in Fig. 5A, the well-ventilated ocean simply cannot supply enough Mn to shallow environments to significantly alter the ε^{205}Tl of the local water masses and, as reducing conditions dissipate, there may be a significant hiatus before Mn-oxide sedimentation is able to recur in these environments. These different scenarios help illustrate how the Tl isotopic response to similar forcings could manifest differently depending upon the overall oxygenation state of the ocean-atmosphere system. Due to these considerations, we propose that the scenario illustrated in Fig. 5B—where the major locus of Mn-oxide formation and burial under lower atmospheric oxygen levels dominantly occurs in shallow marine shelf environments—provides the best explanation for the trends and variability in our Tl data. Importantly, Mn-oxide sediments from these environments have recently been hypothesized to impart smaller Tl isotope fractionations than those formed in deeper waters (Clemente et al., 2025) supporting the notion of a more dynamic Tl cycle that could be locally heterogeneous in its isotopic distribution while still remaining consistent with nearly all the published biogeochemical and paleontological records of the SPICE and later Cambrian oceans (Dahl et al., 2014; Gill et al., 2021; Gill et al., 2011; LeRoy et al., 2021; LeRoy and Gill, 2019; Saltzman et al., 2000; Saltzman et al., 1998; Sheng et al., 2026; Sørensen and Dahl, 2024; Yang et al., 2024; Zhao et al., 2023).

5.4. Controls on interbasinal ε^{205}Tl dynamics

This model for a Tl cycle dominated by shallow-water Mn-oxide generation (Fig. 5B) also provides a reasonable mechanism to explain the differences we record in the absolute values and magnitudes of the changes in ε^{205}Tl between each site. Importantly, this framework

predicts locations nearer the interface between anoxic and oxygenated waters to display wider ranges of values and stronger shifts in ε^{205}Tl as the local water mass rapidly evolves in composition due to vigorous, nearby Mn-oxide generation. As these nearshore waters mix with the open ocean compositions of the distal waters, a gradient of ε^{205}Tl would be established across the basin. Consequently, a more distal location within the anoxic wedge would, at this same time, record the directional shifts in ε^{205}Tl that result from changes near the redox front, but these would be muted in magnitude and shifted toward more negative values relative to a more proximal site. This scenario helps cast this key difference we observe between our records from the Alum Shale and Stockingford Shale Group, as being ultimately caused by the same shoreward expansion of anoxia. In this view, the differences between the ε^{205}Tl records generated at each site are the expected result of the relative basinal position of each, rather than the effect of isolated local processes. While this scenario has not been observed or invoked previously this could be because the studied time period falls within an intermediate marine oxygenation state between Precambrian levels and the full oxygenation of the oceans which has been suggested to have occurred later in the Paleozoic (Dahl et al., 2010; Sperling et al., 2015; Lu et al., 2018; Ostrander et al., 2025).

Another possible explanation for the stratigraphic differences in Tl isotopes between the two localities is basinal restriction. However, due to the lack of evidence for the presence of a sill, including the absence of paleontological or geochemical indicators suggestive of limited water mass exchange, it is not likely that variable hydrographic restriction can account for the recorded Tl isotope values and differences. Furthermore, a restricted basin would have been limited in the supply of available Mn necessary to generate new Mn-oxide formation and sequester enough ^{205}Tl locally to produce the large pre-SPICE negative ε^{205}Tl shift recorded in the Stockingford Shale Group (from −2.0 to −5.2 ε; Fig.4). Importantly, modern restricted basins such as the Black Sea, have sediments that more dominantly reflect riverine inputs of Tl, with ε^{205}Tl values around −2 (Owens, 2019), and this heavy riverine input would also serve to inhibit this shift toward more negative values if the Stockingford Shale was deposited in a restricted basin just prior to the SPICE initiation. It is also important to note that during the positive shift associated with the SPICE onset in the Stockingford Shale (from −5.2 to −0.1 ε; Fig.4) we record values less negative than the bulk input composition of −2 ε^{205}Tl. This seemingly anomalous result suggests that additional ^{205}Tl must have been liberated from the dissolution of local Mn-oxides thereby driving seawater ε^{205}Tl values to compositions more enriched than the bulk input flux. While the shift back to less negative values during the SPICE onset could also reflect increasing basinal restriction, this too is unlikely given a lack of sedimentological, biologic or geochemical evidence for significant change in depositional conditions. Furthermore, it is generally recognized that global sea-level was rising at the time of the early stages of the event (Haq and Schutter, 2008)—a situation which would promote greater basin connectivity to open ocean conditions rather than increasing restriction.

Reexamining our results in this context is particularly illuminating for reconciling the discrepancies we see *both* between our two SPICE records *and* between these records and those of the more recent episodes of marine deoxygenation explored using the ε^{205}Tl proxy (Bowman et al., 2019; Kozik et al., 2023; Kozik et al., 2019; Newby et al., 2021; Ostrander et al., 2017; Them et al., 2018). In particular, we view the Alum Shale record as likely more representative of the global ε^{205}Tl signal across the SPICE, while the Stockingford Shale Group may provide an example of a ε^{205}Tl record from a more shoreward basinal position that imparts a local component to Tl isotope values as a result of intrabasinal manganese cycling, similar to observations made by Ostrander et al. (2020) in their study of Ediacaran Tl dynamics. Our view that the Alum represents open ocean conditions and that the Stockingford records a more nearshore environment is supported by several lines of sedimentary and geochemical evidence. A first-order difference is seen in the stratigraphic thicknesses between the sites, suggesting that the Stockingford Shale Group was deposited in a more nearshore environment, closer to the source of clastic sediment supply. Furthermore, the redox variability seen in Fe-speciation data (LeRoy et al., 2021), suggests an environment with a fluctuating redox gradient potentially close to the boundary of the mixed layer of the upper ocean where atmospheric oxygen permeates and is admixed.

Conversely, the Alum Shale consistently records local anoxia throughout its deposition (Gill et al., 2011) and displays trace metal and isotopic profiles for numerous elements with varying residence times (Gill et al., 2021; Sturesson et al., 2005; Zhao et al., 2023), which suggest the Baltoscandia Basin likely had a consistent hydrographic connection to the adjacent Iapteus Ocean throughout the study interval. This recognition also comports nicely with the view that shallower marine environments were most impacted by the environmental changes associated with the SPICE and that the observed patterns of extinctions were a result of the shoaling of anoxic waters onto the margins of continents (Sørensen and Dahl, 2024; Yang et al., 2024). These observations are consistent with our interpretation of the Tl isotope data, where the expansion of reducing conditions has a much stronger impact on the isotopic response seen in records generated closer to these deoxygenating shallow environments (Stockingford Shale Group). This stronger response, which produced values less negative than riverine input (~ −2 ε^{205}Tl) during the SPICE onset (Fig. 4), was likely driven in part through the local dissolution of previously buried shallow water Mn-oxides, whereas in the distal locations (Alum Shale) the response appears more muted due to the negligible amount of nearby Mn-oxide dissolution. This further illustrates how susceptible shallow marine environments during the earliest Paleozoic were to deoxygenation by relatively small oceanographic changes capable of inducing widespread oxygen-deficient conditions in these shelf regions where significant evolution and diversification of early metazoans is thought to have occurred. This recognition underscores the importance of further understanding how these environmental dynamics may have influenced the trajectory of life on Earth.

6. Conclusions

We investigated changes in the Tl isotopic composition (ε^{205}Tl) of organic-rich, fine-grained clastic rocks deposited before and during the Cambrian SPICE event at locations from the paleocontinents of Baltica (Alum Shale of Sweden) and Avalonia (Stockingford Shale Group of England). Consistent with previous work we record a shift to less negative ε^{205}Tl values associated with the initiation of the SPICE suggesting a reduction in global Mn-oxide burial related to expanding anoxic conditions. Prior to the SPICE we record ε^{205}Tl values which are less negative than the modern ocean value of −6, ranging between about −4 and − 3. This result suggests that the magnitude of the Mn-oxide burial flux was smaller during the Cambrian relative to the modern—a result consistent with previous work and the emerging consensus view that the oceans at this time were less oxygenated as compared to today. This less-oxygenated ocean also appears to have had a significant impact on the dynamics of Mn-oxide cycling in ways that resulted in the early Paleozoic Tl cycle operating differently than in the modern oceans. We report several unique features in our ε^{205}Tl records relative to the canonical view of how Tl behaves in response to marine deoxygenation, that are best understood within the context of these potential differences in early Paleozoic oceanic redox structure. Somewhat surprisingly, we document an initial shift toward more negative ε^{205}Tl values prior to the SPICE (upper Guzhangian Stage) at both of our study locations, a change which we attribute to an enhanced rate of Mn-oxide generation and burial during this time. Additionally, we report differences in the absolute values and magnitude of the shifts in ε^{205}Tl between each site. We argue that both this negative shift, which occurred prior to the typical positive shift documented in numerous Tl isotope studies of deoxygenation episodes, and the differences in absolute values and magnitudes between our two locations, reflects a primary difference in the locus of

Mn-oxide burial during the early Paleozoic compared to the modern ocean. In the Cambrian, Mn-oxides were likely formed predominantly in shallow water environments unlike the modern ocean where they form in extensive regions of the deep sea. This recognition also highlights the potential need to revisit assumptions for the behavior of other isotope systems—such as Mo—that interface with Mn-oxides and may be likewise affected by similar oceanographic dynamics. Given that less-oxygenated oceans have prevailed throughout most of Earth history, this conceptual framework may prove useful for better understanding Tl and Mn cycling in relation to oceanic redox changes across broader swaths of Earth history.

CRediT authorship contribution statement

Matthew A. LeRoy: Investigation, Conceptualization, Writing – original draft. **Benjamin C. Gill:** Resources, Conceptualization, Writing – review & editing. **Sean M. Newby:** Investigation, Writing – review & editing. **Theodore R. Them:** Investigation, Writing – review & editing. **Jeremy D. Owens:** Supervision, Resources, Investigation, Writing – review & editing.

Declaration of competing interest

The authors declare that they have no known competing financial interests or personal relationships that could have appeared to influence the work reported in this paper.

Acknowledgments

The authors would like to thank Vasileios Mavromatis for his editorial guidance and handling of our manuscript. The quality and clarity of this paper was greatly improved by the constructive comments of Wei Wei and another anonymous reviewer. MAL thanks the following providers of financial support for this project: the National Science Foundation Graduate Research Fellowship Program (NSF-GRFP), a student research grant from the Geological Society of America (GSA) and departmental research grants from the Virginia Tech Department of Geosciences. BCG and JDO would like to thank National Aeronautics and Space Administration (80NSSC23K0346). JDO would like to thank National Aeronautics and Space Administration (80NSSC18K1532), and the Sloan Foundation, United States (FG-2020–13552) for funding the elemental work. TRT would like to thank the Florida State University Arts and Sciences Postdoctoral Fellowship. A portion of this work was performed at the National High Magnetic Field Laboratory in Tallahassee, Florida, United States, which is supported by the United States National Science Foundation Cooperative Agreement No. DMR-1644779 and by the State of Florida, United States. Any opinions, findings, and conclusions or recommendations expressed in this material are those of the authors and do not necessarily reflect the views of the NSF.

Appendix A. Supplementary data

Supplementary data to this article can be found online at https://doi.org/10.1016/j.chemgeo.2026.123579.

Data availability

Data will be made available on request.

References

Ahlberg, P., Axheimer, N., Babcock, L.E., Eriksson, M.E., Schmitz, B., Terfelt, F., 2009. Cambrian high-resolution biostratigraphy and carbon isotope chemostratigraphy in Scania, Sweden: first record of the SPICE and DICE excursions in Scandinavia. Lethaia 42, 2–16. https://doi.org/10.1111/j.1502-3931.2008.00127.x.

Bartlett, R., Elrick, M., Wheeley, J.R., Polyak, V., Desrochers, A., Asmerom, Y., 2018. Abrupt global-ocean anoxia during the Late Ordovician–early Silurian detected using uranium isotopes of marine carbonates. Proc. Natl. Acad. Sci. U. S. A. 115, 5896–5901. https://doi.org/10.1073/pnas.1802438115.

Blakey, R.C., 2008. Gondwana paleogeography from assembly to breakup— a 500 m.y. odyssey. In: Fielding, C.R., Frank, T.D., Isbell, J.L. (Eds.), Resolving the Late Paleozoic Ice age in time and space. Geological Society of America.

Bond, D.P.G., Zatoń, M., Wignall, P.B., Marynowski, L., 2013. Evidence for shallow-water 'Upper Kellwasser' anoxia in the Frasnian-Famennian reefs of Alberta, Canada. Lethaia 46, 355–368. https://doi.org/10.1111/let.12014.

Bowman, Chelsie N., Young, S.A., Kaljo, D., Eriksson, M.E., Them II, T.R., Hints, O., Martma, T., Owens, J.D., 2019. Linking the progressive expansion of reducing conditions to a stepwise mass extinction event in the late Silurian oceans. Geology 47, 968–972. https://doi.org/10.1130/G46571.1.

Canfield, D.E., 1998. A new model for Proterozoic Ocean chemistry. Nature 396, 450.

Clarkson, M.O., Kasemann, S.A., Wood, R.A., Lenton, T.M., Daines, S.J., Richoz, S., Ohnemueller, F., Meixner, A., Poulton, S.W., Tipper, E.T., 2015. Ocean acidification and the Permo-Triassic mass extinction. Science 348, 229–232. https://doi.org/10.1126/science.aaa0193.

Clarkson, M.O., Wood, R.A., Poulton, S.W., Richoz, S., Newton, R.J., Kasemann, S.A., Bowyer, F., Krystyn, L., 2016. Dynamic anoxic ferruginous conditions during the end-Permian mass extinction and recovery. Nat. Commun. 7, 12236. https://doi.org/10.1038/ncomms12236.

Clemente, J.N.R., Fan, H., Ostrander, C.M., Zhang, H., Wen, H., Sperling, E.A., Nielsen, S.G., 2025. Thallium isotopes suggest the global deep ocean did not approach modern oxygenation during Cambrian age 3 Metazoan radiation. Geobiology 23, e70028. https://doi.org/10.1111/gbi.70028.

Cole, D.B., Mills, D.B., Erwin, D.H., Sperling, E.A., Porter, S.M., Reinhard, C.T., Planavsky, N.J., 2020. On the co-evolution of surface oxygen levels and animals. Geobiology 1–22. https://doi.org/10.1111/gbi.12382.

Cothren, H.R., Farrell, T.P., Sundberg, F.A., Dehler, C.M., Schmitz, M.D., 2022. Novel age constraints for the onset of the Steptoean positive Isotopic Carbon Excursion (SPICE) and the late Cambrian time scale using high-precision U-Pb detrital zircon ages. Geology. https://doi.org/10.1130/G50434.1.

Cui, Y., Li, M., van Soelen, E.E., Peterse, F., Kürschner, W.M., 2021. Massive and rapid predominantly volcanic CO_2 emission during the end-Permian mass extinction. Proc. Natl. Acad. Sci. 118, e2014701118. https://doi.org/10.1073/pnas.2014701118.

Dahl, T.W., Hammarlund, E.U., Anbar, A.D., Bond, D.P.G., Gill, B.C., Gordon, G.W., Knoll, A.H., Nielsen, A.T., Schovsbo, N.H., Canfield, D.E., 2010. Devonian rise in atmospheric oxygen correlated to the radiations of terrestrial plants and large predatory fish. Proc. Natl. Acad. Sci. 107, 17911–17915. https://doi.org/10.1073/pnas.1011287107.

Dahl, T.W., Boyle, R.A., Canfield, D.E., Connelly, J.N., Gill, B.C., Lenton, T.M., Bizzarro, M., 2014. Uranium isotopes distinguish two geochemically distinct stages during the later Cambrian SPICE event. Earth Planet. Sci. Lett. 401, 313–326.

Dahl, T.W., Siggaard-Andersen, M.-L., Schovsbo, N.H., Persson, D.O., Husted, S., Hougård, I.W., Dickson, A.J., Kjær, K., Nielsen, A.T., 2019. Brief oxygenation events in locally anoxic oceans during the Cambrian solves the animal breathing paradox. Sci. Rep. 9, 1–9. https://doi.org/10.1038/s41598-019-48123-2.

Egenhoff, S.O., Fishman, N.S., Ahlberg, P., Maletz, J., Jackson, A., Kolte, K., Lowers, H., Mackie, J., Newby, W., Petrowsky, M., 2015. Sedimentology of SPICE (Steptoean positive carbon isotope excursion): a high-resolution trace fossil and microfabric analysis of the middle to late Cambrian Alum Shale Formation, southern Sweden. Geol. Soc. Am. Spec. Paper 515, 87–102. https://doi.org/10.1130/2015.2515(05).

Fan, H., Nielsen, S.G., Owens, J.D., Auro, M., Shu, Y., Hardisty, D.S., Horner, T.J., Bowman, C.N., Young, S.A., Wen, H., 2020. Constraining oceanic oxygenation during the Shuram excursion in South China using thallium isotopes. Geobiology 18, 348–365. https://doi.org/10.1111/gbi.12379.

Farrell, T.P., Cothren, H.R., Sundberg, F.A., Schmitz, M.D., Dehler, C.M., Landing, E., Karlstrom, K.E., Crossey, L.J., Hagadorn, J.W., 2025. Revising the late Cambrian time scale and the duration of the SPICE event using a novel Bayesian age modeling approach. GSA Bull. 137, 3093–3118. https://doi.org/10.1130/B37919.1.

Gerhardt, A.M., Gill, B.C., 2016. Elucidating the relationship between the later Cambrian end-Marjuman extinctions and SPICE Event. Palaeogeogr. Palaeoclimatol. Palaeoecol. 461, 362–373.

Gill, B.C., Lyons, T.W., Young, S.A., Kump, L.R., Knoll, A.H., Saltzman, M.R., 2011. Geochemical evidence for widespread euxinia in the later Cambrian Ocean. Nature 469, 80. https://doi.org/10.1038/nature09700.

Gill, B.C., Dahl, T.W., Hammarlund, E.U., LeRoy, M.A., Gordon, G.W., Canfield, D.E., Anbar, A.D., Lyons, T.W., 2021. Redox dynamics of later Cambrian oceans. Palaeogeogr. Palaeoclimatol. Palaeoecol. 581, 110623. https://doi.org/10.1016/j.palaeo.2021.110623.

Hagen, A.P.I., Gill, B.C., Vayda, P.J., Pruss, S.B., 2024. Reconstructing the redox environment of the Cambrian Harkless Formation, Nevada, USA: Navigating the effects of iron-rich clay minerals on the iron speciation redox proxy. Chem. Geol. 670, 122453. https://doi.org/10.1016/j.chemgeo.2024.122453.

Haq, B.U., Schutter, S.R., 2008. A chronology of Paleozoic sea-level changes. Science 322, 64 LP – 68. doi:https://doi.org/10.1126/science.1161648.

Hein, J., Koschinsky, A., 2014. Deep-ocean ferromanganese crusts and nodules. Geochemistry Miner. Depos. Treatise Geochemistry 13, 273–291.

Hlawatsch, S., Neumann, T., van den Berg, C.M.G., Kersten, M., Harff, J., Suess, E., 2002. Fast-growing, shallow-water ferro-manganese nodules from the western Baltic Sea: origin and modes of trace element incorporation. Mar. Geol. 182, 373–387. https://doi.org/10.1016/S0025-3227(01)00244-4.

Jenkyns, H.C., 2010. Geochemistry of oceanic anoxic events. Geochemistry Geophysics Geosystems 11, n/a. https://doi.org/10.1029/2009GC002788.

Kidder, D.L., Worsley, T.R., 2010. Phanerozoic large igneous provinces (LIPs), HEATT (Haline Euxinic Acidic thermal Transgression) episodes, and mass extinctions. Palaeogeogr. Palaeoclimatol. Palaeoecol. 295, 162–191. https://doi.org/10.1016/j.palaeo.2010.05.036.

Koschinsky, A., Hein, J.R., 2017. Marine ferromanganese encrustations: archives of changing oceans. Elements 13, 177–182. https://doi.org/10.2113/gselements.13.3.177.

Kozik, N.P., Young, S.A., Bowman, C.N., Saltzman, M.R., Them, T.R., 2019. Middle–upper Ordovician (Darriwilian–Sandbian) paired carbon and sulfur isotope stratigraphy from the Appalachian Basin, USA: implications for dynamic redox conditions spanning the peak of the Great Ordovician Biodiversification Event. Palaeogeogr. Palaeoclimatol. Palaeoecol. 520, 188–202. https://doi.org/10.1016/j.palaeo.2019.01.032.

Kozik, N.P., Young, S.A., Newby, S.M., Liu, M., Chen, D., Hammarlund, E.U., Bond, D.P. G., Them, T.R., Owens, J.D., 2023. Rapid marine oxygen variability: driver of the late Ordovician mass extinction. Sci. Adv. 8, eabn8345. https://doi.org/10.1126/sciadv.abn8345.

Krause, A.J., Mills, B.J.W., Zhang, S., Planavsky, N.J., Lenton, T.M., Poulton, S.W., 2018. Stepwise oxygenation of the Paleozoic atmosphere. Nat. Commun. 9, 4081. https://doi.org/10.1038/s41467-018-06383-y.

Landing, E., 1983. Highgate gorge: upper Cambrian and Lower Ordovician continental slope deposition and biostratigraphy, Northwestern Vermont. J. Paleo. 57, 1149–1187.

LeRoy, M.A., Gill, B.C., 2019. Evidence for the development of local anoxia during the Cambrian SPICE event in eastern North America. Geobiology 17, 381–400. https://doi.org/10.1111/gbi.12334.

LeRoy, M.A., Gill, B.C., Sperling, E.A., McKenzie, N.R., Park, T.-Y.S., 2021. Variable redox conditions as an evolutionary driver? A multi-basin comparison of redox in the middle and later Cambrian oceans (Drumian-Paibian). Palaeogeogr. Palaeoclimatol. Palaeoecol., 110209 https://doi.org/10.1016/j.palaeo.2020.110209.

Lu, W., Ridgwell, A., Thomas, E., Hardisty, D.S., Luo, G., Algeo, T.J., Saltzman, M.R., Gill, B.C., Shen, Y., Ling, H.-F., Edwards, C.T., Whalen, M.T., Zhou, X., Gutchess, K. M., Jin, L., Rickaby, R.E.M., Jenkyns, H.C., Lyons, T.W., Lenton, T.M., Kump, L.R., Lu, Z., 2018. Late inception of a resiliently oxygenated upper ocean. Science 361, 174–177. https://doi.org/10.1126/science.aar5372.

Meyer, K.M., Kump, L.R., Ridgwell, A., 2008. Biogeochemical controls on photic-zone euxinia during the end-Permian mass extinction. Geology 36, 747–750. https://doi.org/10.1130/G24618A.1.

Newby, S.M., Owens, J.D., Schoepfer, S.D., Algeo, T.J., 2021. Transient Ocean oxygenation at end-Permian mass extinction onset shown by thallium isotopes. Nat. Geosci. 14, 678–683. https://doi.org/10.1038/s41561-021-00802-4.

Newby, S.M., Li, S., Severmann, S., McManus, J., Scholz, F., Owens, J.D., 2025. Refining the signature of thallium isotopes in low oxygen marine environments. Geochim. Cosmochim. Acta 407, 338–356. https://doi.org/10.1016/j.gca.2025.08.020.

Nielsen, A.T., Schovsbo, N.H., 2006. Cambrian to basal Ordovician lithostratigraphy in southern Scandinavia. Bull. Geol. Soc. Denmark 53, 47–92.

Nielsen, A.T., Schovsbo, N.H., 2015. The regressive Early-Mid Cambrian "Hawke Bay Event" in Baltoscandia: Epeirogenic uplift in concert with eustasy. Earth-Science Rev. 151, 288–350. https://doi.org/10.1016/j.earscirev.2015.09.012.

Nielsen, S.G., Mar-Gerrison, S., Gannoun, A., LaRowe, D., Klemm, V., Halliday, A.N., Burton, K.W., Hein, J.R., 2009. Thallium isotope evidence for a permanent increase in marine organic carbon export in the early Eocene. Earth Planet. Sci. Lett. 278, 297–307. https://doi.org/10.1016/j.epsl.2008.12.010.

Nielsen, S.G., Goff, M., Hesselbo, S.P., Jenkyns, H.C., LaRowe, D.E., Lee, C.-T.A., 2011. Thallium isotopes in early diagenetic pyrite – a paleoredox proxy? Geochim. Cosmochim. Acta 75, 6690–6704. https://doi.org/10.1016/j.gca.2011.07.047.

Nielsen, S.G., Prytulak, J., Rehkämper, M., 2017. Investigation and application of thallium isotope fractionation. Rev. Mineral. Geochemistry 82, 759–798. https://doi.org/10.2138/rmg.2017.82.18.

Ostrander, C.M., Owens, J.D., Nielsen, S.G., 2017. Constraining the rate of oceanic deoxygenation leading up to a cretaceous Oceanic Anoxic event (OAE-2: ~94 Ma). Sci. Adv. 3, e1701020. https://doi.org/10.1126/sciadv.1701020.

Ostrander, C.M., Owens, J.D., Nielsen, S.G., Lyons, T.W., Shu, Y., Chen, X., Sperling, E.A., Jiang, G., Johnston, D.T., Sahoo, S.K., Anbar, A.D., 2020. Thallium isotope ratios in shales from South China and northwestern Canada suggest widespread O2 accumulation in marine bottom waters was an uncommon occurrence during the Ediacaran Period. Chem. Geol. 557, 119856. https://doi.org/10.1016/J.CHEMGEO.2020.119856.

Ostrander, C.M., Nielsen, S.G., Gadol, H.J., Villarroel, L., Wankel, S.D., Horner, T.J., Blusztajn, J., Hansel, C.M., 2023. Thallium isotope cycling between waters, particles, and sediments across a redox gradient. Geochim. Cosmochim. Acta 348, 397–409. https://doi.org/10.1016/j.gca.2023.03.028.

Ostrander, C.M., Clemente, J.N.R., Stockey, R.G., Strauss, J.V., Fraser, T., Nielsen, S.G., Sperling, E.A., 2025. Dynamic deep marine oxygenation during the early and Middle Paleozoic. Sci. Adv. 11, eadw5878. https://doi.org/10.1126/sciadv.adw5878.

Owens, J.D., 2019. Application of thallium isotopes. In: Lyons, T.W., Turchyn, A.V., Reinhard, C.T. (Eds.), Elements in Geochemical Tracers in Earth System Science. Cambridge University Press, New York, p. 21. https://doi.org/10.1017/9781108688697.

Owens, J.D., Lyons, T.W., Li, X., Macleod, K.G., Gordon, G., Kuypers, M.M.M., Anbar, A., Kuhnt, W., Severmann, S., 2012. Iron isotope and trace metal records of iron cycling in the proto-North Atlantic during the Cenomanian-Turonian oceanic anoxic event (OAE-2). Paleoceanography 27. https://doi.org/10.1029/2012PA002328.

Owens, J.D., Nielsen, S.G., Horner, T.J., Ostrander, C.M., Peterson, L.C., 2017. Thallium-isotopic compositions of euxinic sediments as a proxy for global manganese-oxide burial. Geochim. Cosmochim. Acta 213, 291–307. https://doi.org/10.1016/j.gca.2017.06.041.

Ozaki, K., Tajika, E., 2013. Biogeochemical effects of atmospheric oxygen concentration, phosphorus weathering, and sea-level stand on oceanic redox chemistry: Implications for greenhouse climates. Earth Planet. Sci. Lett. 373, 129–139. https://doi.org/10.1016/j.epsl.2013.04.029.

Peng, Y.Y., Peng, Y.Y., Lang, X., Ma, H., Huang, K., Li, F., Shen, B., 2016. Marine carbon-sulfur biogeochemical cycles during the Steptoean positive Carbon Isotope Excursion (SPICE) in the Jiangnan Basin, South China. J. Earth Sci. 27, 242–254. https://doi.org/10.1007/s12583-016-0694-4.

Pruss, S.B., Gill, B.C., 2024. Life on the edge: the Cambrian marine realm and oxygenation. Annu. Rev. Earth Planet. Sci. 52, 109–132.

Pruss, S.B., Jones, D.S., Fike, D.A., Tosca, N.J., Wignall, P.B., 2019. Marine anoxia and sedimentary mercury enrichments during the Late Cambrian SPICE event in northern Scotland. Geology 47, 1–4. https://doi.org/10.1130/G45871.1.

Rehkämper, M., Nielsen, S.G., 2004. The mass balance of dissolved thallium in the oceans. Mar. Chem. 85, 125–139. https://doi.org/10.1016/j.marchem.2003.09.006.

Rooney, A.D., Millikin, A.E.G., Ahlberg, P., 2022. Re-Os geochronology for the Cambrian SPICE event: Insights into euxinia and enhanced continental weathering from radiogenic isotopes. Geology 50, 716–720. https://doi.org/10.1130/G49833.1.

Rushton, A.W.A., 1978. Fossils from the Middle–Upper Cambrian transition in the Nuneaton district. Palaeontology 21, 245–283.

Rushton, A.W.A., 1983. Trilobites from the Upper Cambrian Olenus Zone in Central England. Spec. Pap. Palaeontol. 30, 107–139.

Saltzman, M.R., Runnegar, B., Lohmann, K.C., 1998. Carbon isotope stratigraphy of Upper Cambrian (Steptoean Stage) sequences of the eastern Great Basin: Record of a global oceanographic event. Geol. Soc. Am. Bull. 110, 285–297. https://doi.org/10.1130/0016-7606(1998)110<0285:cisouc>2.3.co;2.

Saltzman, M.R., Ripperdan, R.L., Brasier, M.D., Lohmann, K.C., Reichart, R.A., Chang, W. T., Peng, S., Ergaliev, E.K., Runnegar, B., 2000. A global carbon isotope excursion (SPICE) during the late Cambrian: relation to trilobite extinctions, organic-matter burial and sea level. Palaeogeogr. Palaeoclimatol. Palaeoecol. 162, 211–223 doi: papers3://publication/uuid/542545CA-6777-4D59-B0EA-2F7E40517D9F.

Saltzman, M.R., Young, S.A., Kump, L.R., Gill, B.C., Lyons, T.W., Runnegar, B., 2011. Pulse of atmospheric oxygen during the late Cambrian. Proc. Natl. Acad. Sci. 108. https://doi.org/10.1073/pnas.1011836108.

Saltzman, M.R., Edwards, C.T., Adrain, J.M., Westrop, S.R., 2015. Persistent oceanic anoxia and elevated extinction rates separate the Cambrian and Ordovician radiations. Geology 43, 807–810. https://doi.org/10.1130/G36814.1.

Schiffbauer, J.D., Huntley, J.W., Fike, D.A., Jeffrey, M.J., Gregg, J.M., Shelton, K.L., 2017. Decoupling biogeochemical records, extinction, and environmental change during the Cambrian SPICE event. Sci. Adv. 3.

Schulz, H.-M., Yang, S., Schovsbo, N.H., Rybacki, E., Ghanizadeh, A., Bernard, S., Mahlstedt, N., Krüger, M., Amann-Hildebrandt, A., Krooss, B.M., Meier, T., Reinicke, A., 2021. The Furongian to lower Ordovician Alum Shale Formation in conventional and unconventional petroleum systems in the Baltic Basin – a review. Earth-Science Rev. 218, 103674. https://doi.org/10.1016/j.earscirev.2021.103674.

Sheng, K., Li, Z.-H., Zhou, J.-L., Lin, Y.-B., Xiong, G.-L., Ren, G.-Y., Chen, Z.-Q., Lenton, T. M., Shen, S., Zhang, F., 2026. Earth system instability explains redox paradox during late Cambrian SPICE event. Sci. Adv. 12, eaeb9224. https://doi.org/10.1126/sciadv.aeb9224.

Sørensen, A.L., Dahl, T.W., 2024. Cascading oxygen loss shoreward in the oceans: Insights from the Cambrian SPICE event. One Earth 7, 1108–1120. https://doi.org/10.1016/j.oneear.2024.05.011.

Sperling, E.A., Wolock, C.J., Morgan, A.S., Gill, B.C., Kunzmann, M., Halverson, G.P., Macdonald, F.A., Knoll, A.H., Johnston, D.T., 2015. Statistical analysis of iron geochemical data suggests limited late Proterozoic oxygenation. Nature 523, 451.

Stolper, D.A., Keller, C.B., 2018. A record of deep-ocean dissolved O2 from the oxidation state of iron in submarine basalts. Nature. https://doi.org/10.1038/nature25009.

Sturesson, U., Popov, L.E., Holmer, L.E., Bassett, M.G., Felitsyn, S., Belyatsky, B., 2005. Neodymium isotopic composition of Cambrian–Ordovician biogenic apatite in the Baltoscandian Basin: implications for palaeogeographical evolution and patterns of biodiversity. Geol. Mag. 142, 419–439. https://doi.org/10.1017/S0016756805000877.

Them, T.R., Gill, B.C., Caruthers, A.H., Gerhardt, A.M., Gröcke, D.R., Lyons, T.W., Marroquín, S.M., Nielsen, S.G., Alexandre, J.P.T., Owens, J.D., Them, T.R., Gill, B.C., Caruthers, A.H., Gerhardt, A.M., Gröcke, D.R., Lyons, T.W., Marroquín, S.M., Nielsen, S.G., Trabucho Alexandre, J.P., Owens, J.D., Theodore R. Them, I.I., Gill, B. C., Caruthers, A.H., Gerhardt, A.M., Gröcke, D.R., Lyons, T.W., Marroquín, S.M., Nielsen, S.G., Alexandre, J.P.T., Owens, J.D., Them, T.R., Gill, B.C., Caruthers, A.H., Gerhardt, A.M., Gröcke, D.R., Lyons, T.W., Marroquín, S.M., Nielsen, S.G., Trabucho Alexandre, J.P., Owens, J.D., Theodore R. Them, I.I., Gill, B.C., Caruthers, A.H., Gerhardt, A.M., Gröcke, D.R., Lyons, T.W., Marroquín, S.M., Nielsen, S.G., Alexandre, J.P.T., Owens, J.D., Them, T.R., Gill, B.C., Caruthers, A.H., Gerhardt, A. M., Gröcke, D.R., Lyons, T.W., Marroquín, S.M., Nielsen, S.G., Trabucho Alexandre, J.P., Owens, J.D., Theodore R. Them, I.I., Gill, B.C., Caruthers, A.H., Gerhardt, A.M., Gröcke, D.R., Lyons, T.W., Marroquín, S.M., Nielsen, S.G., Alexandre, J.P.T., Owens, J.D., Them, T.R., Gill, B.C., Caruthers, A.H., Gerhardt, A. M., Gröcke, D.R., Lyons, T.W., Marroquín, S.M., Nielsen, S.G., Trabucho Alexandre, J.P., Owens, J.D., Them, T.R., Gill, B.C., Caruthers, A.H., Gerhardt, A.M., Gröcke, D.R., Lyons, T.W., Marroquín, S.M., Nielsen, S.G., Alexandre, J.P.T., Owens, J.D., 2018. Thallium isotopes reveal protracted anoxia during the Toarcian (Early Jurassic) associated with volcanism, carbon burial, and mass extinction. Proc. Natl. Acad. Sci. 115, 6596–6601. https://doi.org/10.1073/pnas.1803478115.

Thompson, C.K., Kah, L.C., 2012. Sulfur isotope evidence for widespread euxinia and a fluctuating oxycline in Early to Middle Ordovician greenhouse oceans. Palaeogeogr.

Palaeoclimatol. Palaeoecol. 313–314, 189–214. https://doi.org/10.1016/j.palaeo.2011.10.020.
Wang, Y., Lu, W., Costa, K.M., Nielsen, S.G., 2022. Beyond anoxia: Exploring sedimentary thallium isotopes in paleo-redox reconstructions from a new core top collection. Geochim. Cosmochim. Acta 333, 347–361. https://doi.org/10.1016/j.gca.2022.07.022.
Wignall, P.B., 2001. Large igneous provinces and mass extinctions. Earth Sci. Rev. 53, 1–33. https://doi.org/10.1016/S0012-8252(00)00037-4.
Wignall, P.B., Twitchett, R.J., 1996. Oceanic anoxia and the end Permian mass extinction. Science 272, 1155–1158. https://doi.org/10.1126/science.272.5265.1155.
Woods, M.A., Wilby, P.R., Leng, M.J., Rushton, A.W.A., Williams, M., 2011. The Furongian (late Cambrian) Steptoean positive Carbon Isotope Excursion (SPICE) in Avalonia. J. Geol. Soc. Lond. 168, 851–862. https://doi.org/10.1144/0016-76492010-111.
Wotte, T., Strauss, H., 2015. Questioning a widespread euxinia for the Furongian (late Cambrian) SPICE event: indications from δ13C, δ18O, δ34S and biostratigraphic constraints. Geol. Mag. 152, 1085–1103. https://doi.org/10.1017/S0016756815000187.
Yang, A., Chen, B., Sun, Z., Tostevin, R., He, T., Chen, X., Chen, Jitao, Lu, M., Hu, C., Du, S., Chen, Jun, Jiao, W., Zhu, M., 2024. Shallow Ocean deoxygenation drove trilobite turnover during the late Cambrian SPICE event. Geology 52, 661–666. https://doi.org/10.1130/G52200.1.
Zhang, F., Dahl, T.W., Lenton, T.M., Luo, G., Shen, S., Algeo, T.J., Planavsky, N., Liu, J., Cui, Y., Qie, W., Romaniello, S.J., Anbar, A.D., 2020. Extensive marine anoxia associated with the Late Devonian Hangenberg Crisis. Earth Planet. Sci. Lett. 533, 115976. https://doi.org/10.1016/j.epsl.2019.115976.
Zhao, Z., Ahlberg, P., Thibault, N., Dahl, T.W., Schovsbo, N.H., Nielsen, A.T., 2022. High-resolution carbon isotope chemostratigraphy of the middle Cambrian to lowermost Ordovician in southern Scandinavia: implications for global correlation. Glob. Planet. Change 209, 103751. https://doi.org/10.1016/j.gloplacha.2022.103751.
Zhao, Z., Pang, X., Zou, C., Dickson, A.J., Basu, A., Guo, Z., Pan, S., Nielsen, A.T., Schovsbo, N.H., Jing, Z., Dahl, T.W., 2023. Dynamic oceanic redox conditions across the late Cambrian SPICE event constrained by molybdenum and uranium isotopes. Earth Planet. Sci. Lett. 604, 118013. https://doi.org/10.1016/j.epsl.2023.118013.